macQsimal	Title **MEMS cells characterization report**	Deliverable Number **D5.3**
Project Number **820393**		Version **1**

H2020-FETFLAG-2018-2021

macQsimal

Miniature Atomic vapor-Cell Quantum devices for SensIng and Metrology AppLications

Deliverable D5.3

MEMS cells characterization report

WP5 – Miniature atomic clocks

Authors: Saba Zabihzadeh, Sylvain Karlen, Thomas Overstolz, Jacques Haesler (CSEM)

Lead participant: CSEM

Delivery date: 31.07.2022

Dissemination level: Public

Type: R (Document, Report)

This work has received funding from the European Union's Horizon 2020 research and innovation programme under grant agreement No. 820393.

Revision History

Author Name, Partner short name	Description	Date
Sylvain Karlen (CSEM)	Draft deliverable	01.06.2022
Saba Zabihzadeh (CSEM)	Lifetime calculation and estimation	01.07.2022
Thomas Overstolz (CSEM)	Additional inputs and first review	12.07.2022
Jacques Haesler (CSEM)	Final review	14.07.2022
Johannes Ripperger (accelCH)	Final formal checks and formatting	31.07.2022

Abbreviations

MAC	Miniature Atomic Clock
MEMS	Micro Electro-Mechanical Systems
UV	Ultraviolet
WP	Work Package

Partner short names

accelCH	accelopment Schweiz AG, CH
CSEM	CSEM SA – Centre Suisse d'Électronique et de Microtechnique, CH
SPT	Orolia Switzerland SA (Spectratime), CH
UNINE	Université de Neuchâtel, CH

Contents

1 Introduction

One of the applications of micro-fabricated (MEMS) alkali vapor cells is in the domain of atomic clocks, known as Miniaturized Atomic Clocks or MAC cells. During the macQsimal project, a great progress has been made in terms of cell manufacturing process, filling, and UV decomposition techniques. The fabrication details of these cells are discussed in deliverable D3.3. One important criterion for the MEMS based vapor cells is related to their lifetime. To demonstrate the real potential of these vapor cells, a lifetime estimation of 10 years under operation condition (95°C) is required.

This deliverable describes in detail the different methods employed in the frame of the macQsimal project to characterize the MEMS vapor cells. Techniques such as Raman spectroscopy, optical microscopy, and white light interferometry were employed. The experimental approaches and statistical models applied for a lifetime study of the RbN_3-filled MEMS cells remain at the focus of this document.

2 Heater resistance measurement

The characterization of the Pt resistive heater integrated on the MEMS vapor cells was treated in detail in the report related with the deliverable D3.3.

3 MAC cells lifetime calculation and estimation

3.1 Introduction

One of the important questions about the miniaturized Rb atomic clock concerns their lifetime at operation temperature, i.e., 10 years of lifetime at 95°C is demanded for MAC cells.

Metallic Rb and N_2 buffer gas are created inside the cells after UV-decomposition of deposited rubidium-azide (RbN_3). The decomposition reaction is explained in equation 1. The decomposition is UV activated.

$$2\,RbN_3 \rightarrow 2Rb + 3N_2 \qquad \textit{Equation 1}$$

This filling method has the advantage of being low cost. However, the amount of Rb is directly linked to the amount of N_2 present in the cell. Typically, a total buffer gas pressure in the order of 140 mbar (Ar + N_2 at room temperature) is required in a MEMS cell used for atomic clock. The required ratio between Ar and N_2 is given by the temperature of the cell operation. Each of the two gases adds a thermal dependence of the clock frequency to the temperature. Ar and N_2 having coefficients of opposite signs, it is possible to cancel-out the first order dependency of the clock frequency to the cell temperature by choosing an appropriate ratio between the two gases. For an operation temperature of 95°C, an Ar to N_2 ratio in the order of 1.3 is required. This corresponds to a partial pressure of N_2 in the order of 50 mbar at room temperature.

The constraint on the N_2 pressure limits the amount of Rb to approximately 1.2µg for a cell with a cavity diameter of 3mm and a cavity depth of 1.5mm. Once the available amount of Rb is consumed by one of the different failure mechanisms involved, no Rb spectra can be measured anymore, and the atomic clock fails.

Performing accelerated aging of the MEMs cells after UV decomposition allows us to estimate the Rb consumption rate at elevated temperature. This process is linked through the Arrhenius equation to the activation energy of the Rb loss mechanism. A correlation can hence be established between the Rb consumption process at elevated temperature and the temperature of operation, allowing us to retrieve the expected lifetime of the vapor cell under normal condition of operation.

3.2 Rb consumption mechanism

Metallic Rb consumption inside the MEM cells occurs in two steps:

1) Initial Rb consumption: which occurs just after decomposition of rubidium-azide (RbN_3) by UV irradiation.
2) Rb consumption during thermal aging test; the consumption rate depends on the testing temperature

The initial loss of Rb can be partially explained by its reaction with some contamination on the cell surface or volume (i.e., oxygen).

On the other hand, the mechanism of the second step Rb consumption is not very well understood, especially for the cells with internal barrier layers. For the cells without any coating (barrier) layer, Rb consumption by time and temperature can be described by two possible candidate processes:

1) reduction of the sodium oxide contained in the glass or of the glass silicon dioxide by the rubidium; in this case the consumed mass is proportional to time
2) diffusion of the rubidium in the bulk of the glass; in which the consumption mass is proportional to √t; diffusion law.

Diffusion of the Rb inside the glass substrate is reduced dramatically by coating the cell internal surface with a barrier layer such as amorphous Al_2O_3. Extremely slow reduction of the Al_2O_3 layer by the rubidium or diffusion of Rb to the glass through pinholes in the Al_2O_3 layer are two possible explanations of Rb loss in Al_2O_3 coated cells. By considering a constant consumption rate while the consumption mass is linearly proportional to the time, the remaining metallic Rb inside these cells is calculated as follows:

$$m_{meas.}(t) = m_{prod.} - m_{init.\ cons.} - k \cdot t \qquad \textit{Equation 2}$$

Here, $m_{prod.}$ and $m_{init.\ cons.}$ are, respectively, the mass of Rb produced by UV decomposition of RbN_3 (nominal weight), and the mass of initial Rb consumption.

3.3 Rb consumption monitoring

Direct monitoring of the metallic Rb consumption can be done based on the image analysis of the Rb droplets at the surface of the MEMS atomic cells while going through the thermal aging. By cooling the cells to the ambient temperature, thermal gradient results in formation and migration of the Rb droplets to the internal top window of the cells. The cell imaging is done using a confocal microscope, and the radius of the droplets is calculated using an image recognition software. Figure 3-1 shows the evolution of Rb droplets in a MAC cell while undergoing thermal aging at 195°C.

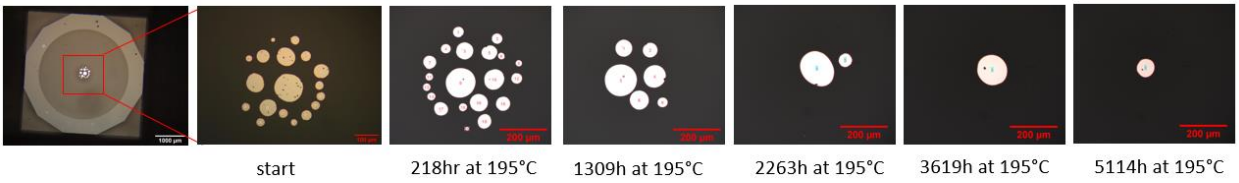

Figure 3-1: Evolution of Rb droplet inside a vapor cell at different intervals while performing thermal aging at 195°C.

Knowing the radius of the droplet (a), allows calculation of the volume (V) by estimation of a contact angle (θ); as explained below. The contact angle depends mainly on the wettability of Rb on Al_2O_3 coated surface.

$$V = \frac{\pi h}{6}(3a^2 + h^2) \quad h = a\tan(\theta/2) \qquad \textit{Equation 3}$$

Figure 3-2 displays a schematic drawing of the spherical cap explaining the relation between the calculate volume and the measured radius in the optical image.

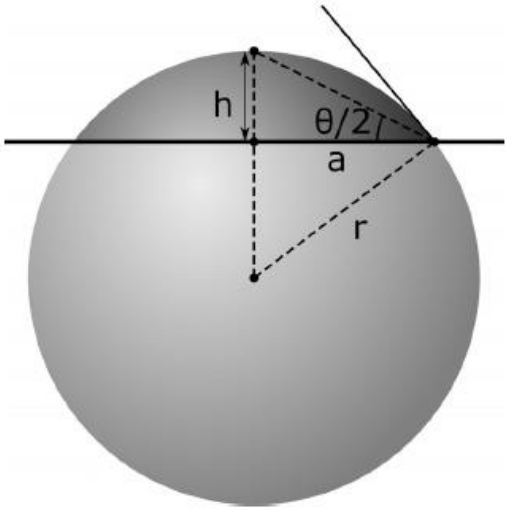

Figure 3-2: Schematic drawing of a spherical cap used for Rb drop volume estimation from the optical image.

The Rb mass is finally calculated from the estimated volume and the density of metallic rubidium.

3.4 Calibration of the contact angle

Different approaches are employed for the estimation of the contact angle. The details are explained in this section. Different values are estimated for the contact angle using different approaches. These differences are partially originating from the large scattering in cells behaviour and (experimental) error bar of each employed method.

3.4.1 Rb mass estimation from optical images: cells without initial thermal treatment

The contact angle is calibrated from the measured mass of Rb inside the cells and the initial Rb consumption. For this purpose, several cells filled with different RbN_3 quantities were decomposed by UV. Then, the amount of the Rb inside the cells was evaluated using optical image analysis as explained earlier. The initial consumption is estimated from the difference between the theoretical produced and measured mass of the metallic Rb inside the cell.

The produced mass of metallic Rb inside the cell is calculated from the stoichiometric relation between N_2 and Rb after UV decomposition of the rubidium azide. For this calculation the impurity of the RbN_3 as well as the UV decomposition yield of the RbN_3 solution should be considered. Then, the contact angle is used in a way in which the slope between the measured mass and nominal mass becomes close to 1.

Impurities and the decomposition yield of the cells can be estimated from N_2 pressure inside the MAC cells (see section 3.6.). For ID20200616 cell series, in total 75 cells were selected for accelerated thermal aging tests. To estimate the correct contact angle, cells with different RbN_3 filling were selected and their initial Rb was estimated using the optical microscope.

3.4.2 Calibration of the Rb nominal weight

To increase the accuracy of the estimated Rb nominal weight, the N_2 pressure inside 40 cells (20 cells with ^{87}Rb and 20 cells containing ^{nat}Rb) were measured using Raman spectroscopy, and the nominal Rb weight was calibrated based on the averaged calculated yield. The employed approach for N_2 pressure estimation is explained later in section 3.6. An average yield/impurity of 95.6% ± 5.8% and 88.8% ± 9% has been estimated respectively for cells containing ^{87}Rb and ^{nat}Rb. Figure 3-3 displays the measured N_2 pressure as of the measured cells the function of the theoretical pressure for 100% yield. A better decomposition yield/purity is obtained for cells filled with ^{87}Rb type. Maximum of the peak intensity has been calculated using spline interpolation. As can be seen, a lower decomposition yield/ purity is obtained for cells filled with nat-Rb.

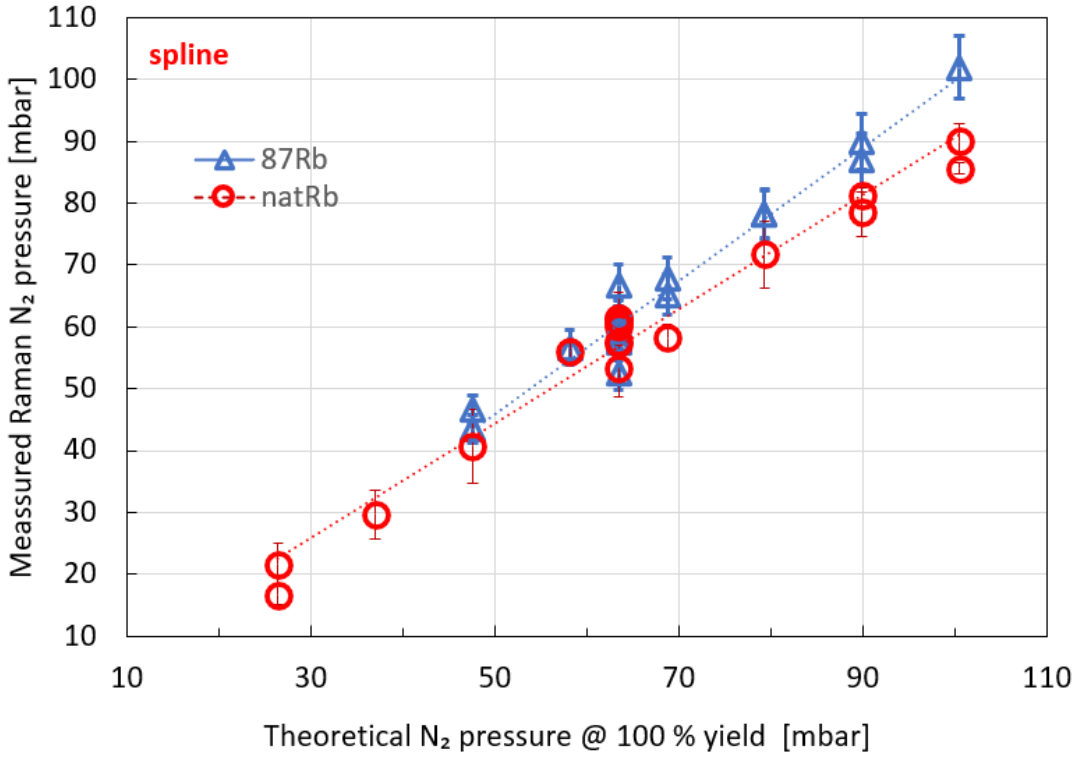

Figure 3-3: Measured N_2 pressure inside ID20200616 cells using Raman spectroscopy as the function of the expected N_2 pressure while considering a 100% decomposition and 100% purity.

Figure 3-4 displays the variation of the optically measured weight as the function of the nominal weight for cells with ^{87}Rb and ^{nat}Rb. The nominal weight on the X-axis has been calibrated based on the calculated N_2 pressure from Raman spectroscopy. For the cells in which the pressure hasn't been measured, the estimated value of 90% of the yield has been selected; based on previously measured impurity using XRD method. To improve the accuracy in the optically measured radius of Rb droplet, all cells went through 72h at 195°C initial thermal aging. To be coherent between the cells with both ^{87}Rb and nat-Rb, the line fitting has been done on the cells with a filling larger than 14nl. More details about this method are explained in section 3.4.5.

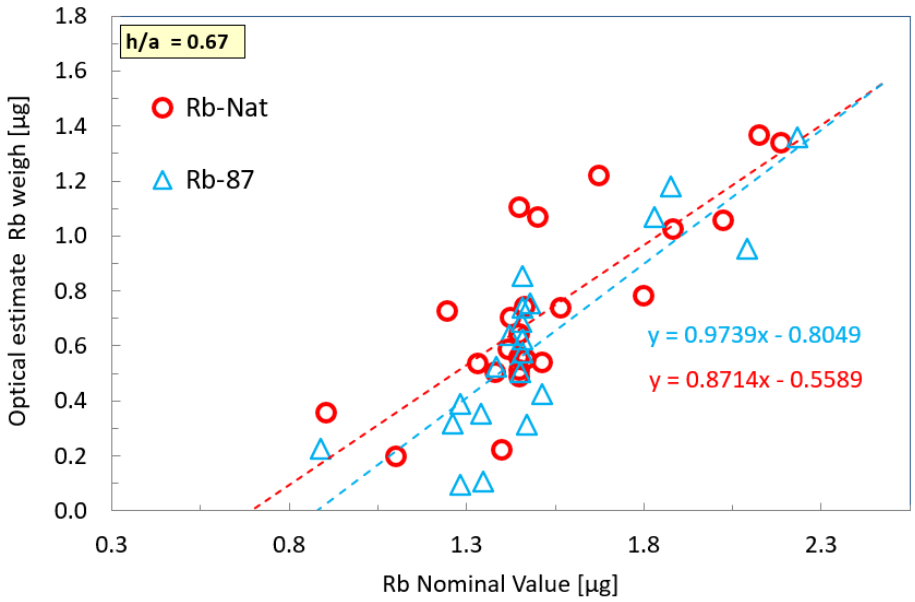

Figure 3-4: Variation of the estimated mass from optical images and the expected produced mass for ID20200616 cells (yield decomposition / impurity 90%).

A noticeable difference is observed between the slope calculated for ^{87}Rb and nat-Rb type. This difference is partially explained by the accuracy in the optical measurement of the droplet's diameters, the large scattering in the data, the experimental error, and the large scattering in the Raman measurement. A lower decomposition yield and / or higher impurity may be considered as another source of the observed differences. A contact angle of 68° (h/a =0.67) results in a slope close to 1 for this graph for ^{87}Rb cells.

3.4.3 Calculation of the contact angle using a white-light interferometer

The diameter and the height of the Rb droplets was measured as well using a white-light interferometer. For this purpose, two different cells were selected: from 2mm and 3mm diameter series.

The results are presented in Figure 3-5. Using the interferometer data S08 cell (2mm diameter, with MVD coated AlOx layer) and E11 cell (3mm diameter, with ALD coated AlO_x layer), respectively h/a of (0.55 $\pm$ 0.04) and (0.46 $\pm$ 0.12) has been calculated. As can be seen, the accuracy of the measured h/a value depends strongly on the image quality and varies between the droplets.

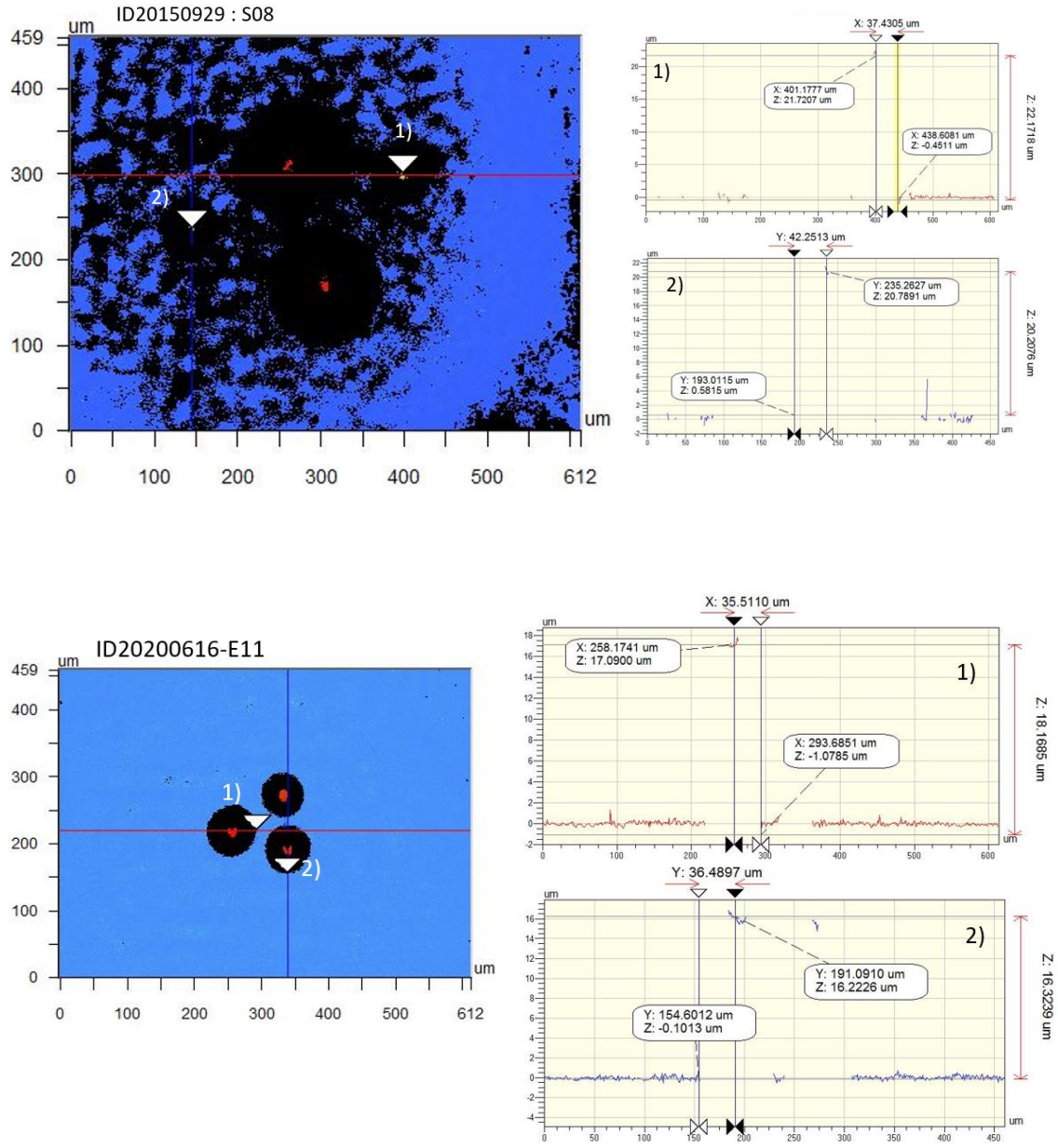

Figure 3-5: Height and dimeter of metallic Rb droplets inside the cells measured with a white-light interferometer.

3.4.4 Contact angle: published value in the literature

Considering the large differences between the contact angles calculated from different methods, for this part of the project, the published value for contact angle in the work of Karlen *et al.* (57°, h/a =0.54) has been selected for this project; this contact angle is obtained for 2mm diameter cells from ID20150929 wafer series. It should be noted that for these cells a very good agreement has been obtained between different employed methods for the estimation of the contact angle.

It is important to mentioned that the lifetime estimation of the MAC cells is independent of the selected contact angle, as far as this value remains the same along the whole calculations. More explanation can be found in section 3.7.1.

3.4.5 Impact of the initial thermal treatment on observed Rb droplets and calibrated contact angle

The developed protocol (explained in section 3.3) depends strongly on the image contrast and the defined threshold for a correct estimation of droplet diameter. Consequently, the error increases for cells with larger number of Rb droplets. One of the approaches to minimize the error is performing initial thermal treatment for few days. Initial thermal treatment allows migration of the smaller droplets to bigger ones and results in decreasing the measured error.

For cells with wafer identification ID20200616, some cells with 24nl filling were selected and treated for 72hrs at 178°C. The increase in the optically estimated weight of metallic Rb is shown in Figure 3-6; here the results are shown for a contact angle of 57°. It should be considered, that although initial thermal treatment results in a better estimation of the initial Rb weight, it decreases the cell lifetime, as they went through accelerated thermal aging for few days.

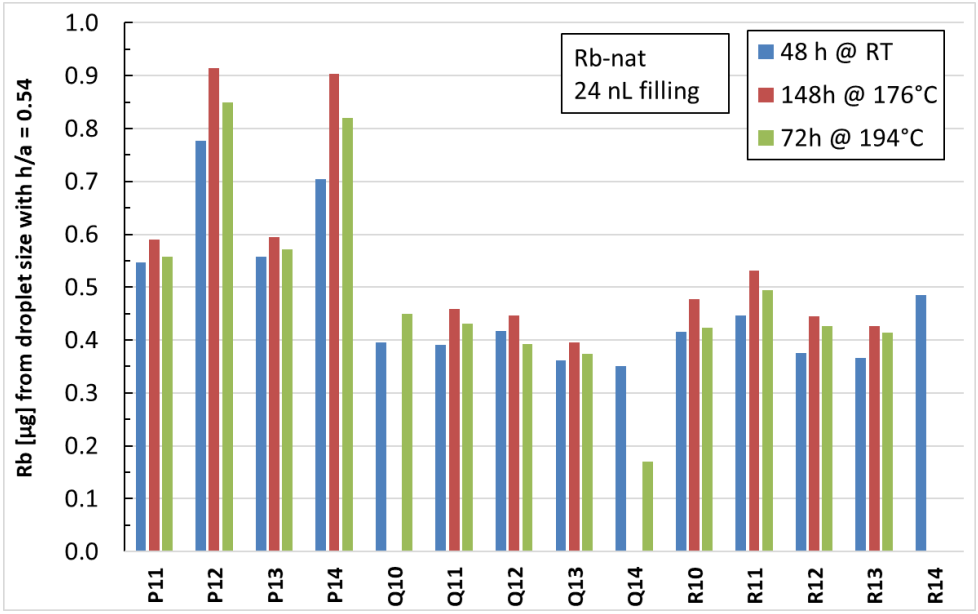

Figure 3-6: Impact of the initial thermal treatment on the optically measured value of metallic Rb weight, from the observed droplets on the optical microscope.

The impact of initial thermal treatment on the optically observed metallic Rb weight was measured as well for ID20201019 MAC cells. For this purpose, the cells were heated for 72hr at 195°C. The histogram distribution of a change in the measured value of Rb weight after thermal treatment is shown at left in Figure 3-7, the accumulative distribution is presented at right in Figure 3-7.

As can be seen in Figure 3-7, the thermal treatment mainly results in an increase in the optically estimated Rb mass of up to 50% in some cells, while few cells show a decrease of the Rb mass. As explained earlier, an increase in the estimated Rb weight from optical images after initial thermal treatment is due to migration of smaller droplet to the bigger ones. Decreasing the number of droplets results in a decrease in the error of grey-level threshold estimation in image treatment. On the other hand, initial thermal treatment at elevated temperature is considered as well as the beginning of accelerated thermal aging and consequently Rb consumption.

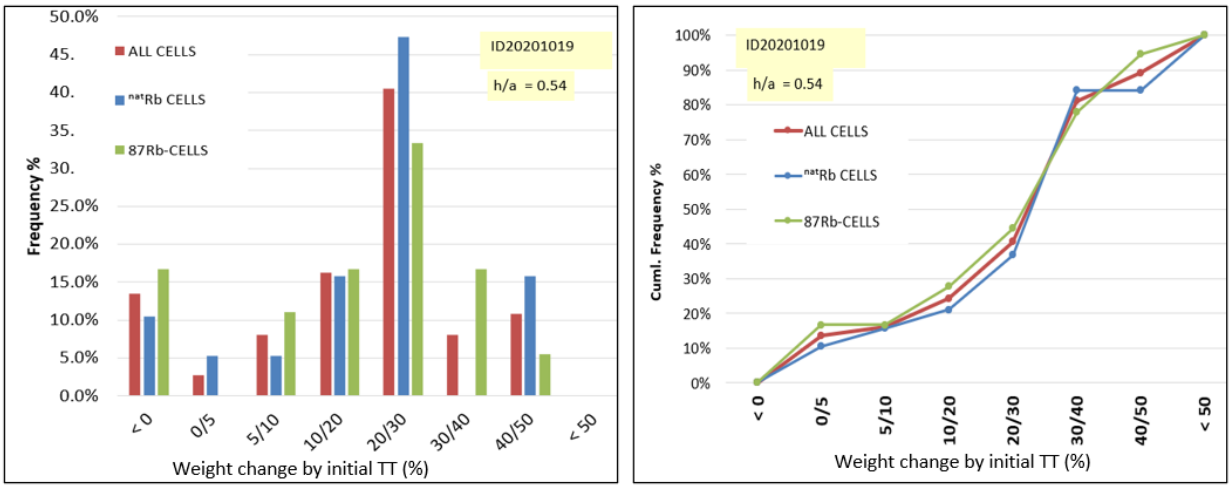

Figure 3-7: histogram (left) and accumulative distribution (right) of change in optically measured Rb metallic weight after 72 hours of thermal treatment at 195°C.

3.5 Initial loss of Rb

By considering a contact angle of 57° for Rb metallic droplets, the estimated yield from N_2 pressure gives an initial loss of 0.983±0.2 and 0.883±0.26 respectively for ^{87}Rb and ^{nat}Rb, without going through any initial TT. As previously mentioned, an average yield of 90% was considered for the cells in which the N_2 pressure has not been measured. The data scattering has been calculated from the standard deviation of the measured data. The statistical distribution of the Rb initial loss has been calculated as well for ID20200616 cells, and the results for both histogram distribution and accumulative value are shown in Figure 3-8 a and b respectively.

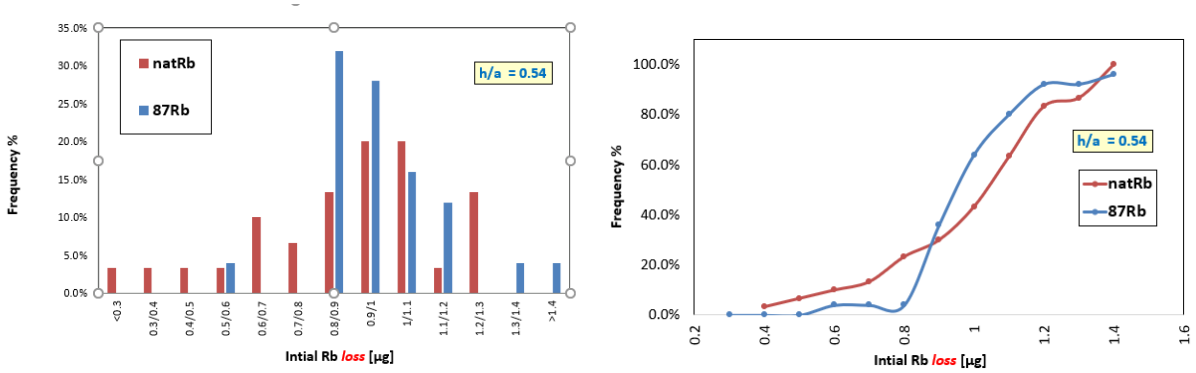

Figure 3-8: The histogram distribution of Rb initial loss for cells from ID20200616 series.

3.6 Quantitative Micro-Raman Spectroscopy for Partial Pressure Measurement in MEMs cells

Raman spectroscopy is a non-destructive method which is used to calculate the pressure inside the MAC cells. The measurements are performed using a LABRAM Micro-Raman from Horiba equipped with green laser; 532nm wavelength. For this measurement, the laser is focalized inside the cell cavity. The N_2

pressure is calculated from the Raman peak intensity generated by nitrogen molecules (at 2328 cm^{-1}) inside the cell.

The intensity of the Raman peaks of the gas is proportional to their pressure as explained in Equation 4, in which I (v), I_0, σ(v) and p correspond respectively to the Raman intensity of the gas, laser intensity, Raman cross section and gas partial pressure.

$$I(\upsilon) \propto I_0\, \sigma(\upsilon) p \qquad \textit{Equation 4}$$

For this measurement, first the intensity of the N_2 peak (at 2328 cm^{-1}) is measured inside a broken cell filled with atmospheric pressure (≈761mbar); 1 atm. Then, Raman experiment is done on a cell filled only with Ar gas (without any RbN_3 filling) that allows us measuring the N_2 signal produced from the interaction of the laser with N_2 present in the instrument's atmosphere (outside the cell); I_{Ar}. Finally, Raman intensity of a cell after UV decomposition of RbN_3 is measured (I_{cell}). The pressure inside the cell is calculated from as below, after calibration of the peak intensity for the measured pressure. There exist several methods for peak intensity estimation: 1) taking the maximum value of the measured peak intensity, 2) applying spline interpolation and 3) taking the maximum intensity value of the split-Pearson function fitted on the measured data.

$$p_{\mathrm{N_2,cell}} = \frac{I_{\mathrm{cell}} - I_{\mathrm{Ar}}}{I_{\mathrm{atm.}} - I_{\mathrm{Ar}}} p_{\mathrm{N_2,atm.}} \qquad \textit{Equation 5}$$

Measuring the N_2 pressure using Raman spectroscopy is considered as well as an indirect control method on the RbN_3 filling inside the cells. Figure 3-9 displays the N_2 pressure measured using Raman spectroscopy inside 5 cells from ID20200929 series. In the presented graph, the results are compared with N_2 pressure obtained from atomic spectroscopy Vernier and Bean estimations. The Raman measurement was repeated three times for each cell, data scattering is presented as error bar inside the graph. Filling value of RbN_3 inside each cell has been mentioned as well in Y-axis. A reasonable agreement has been obtained between N_2 pressure measured by Raman and Vernier estimation. Here, the peak intensity has been selected simply by taking the maximum intensity value of the measured data.

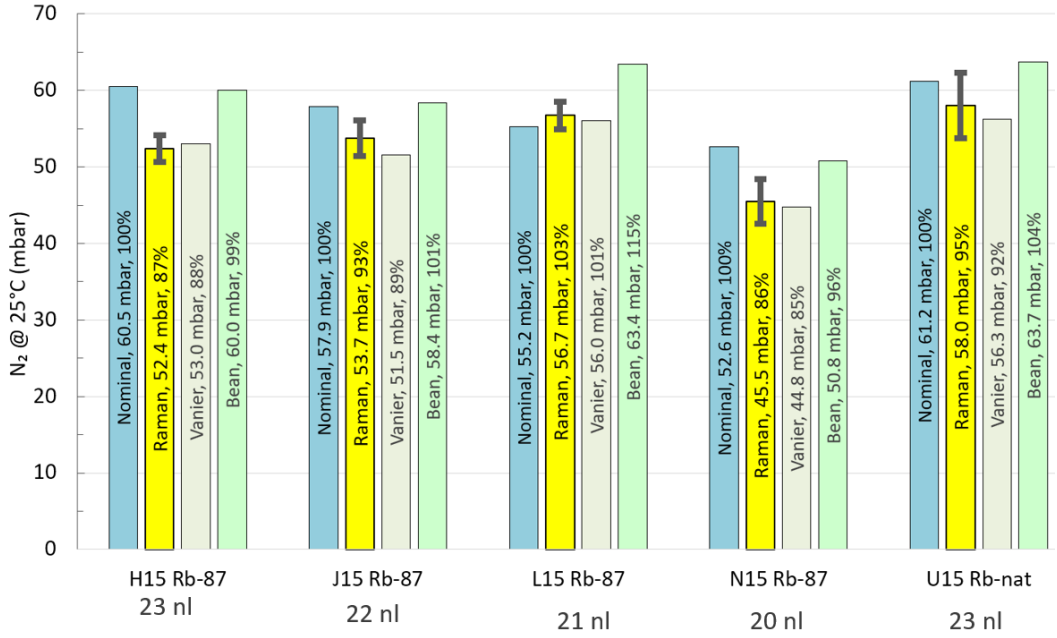

Figure 3-9: N_2 pressure measured inside 5 cells from ID20200616 series using different methods.

Calculated N_2 pressure using Raman spectroscopy indicate a purity in the range of 86 to 100% for the employed RbN_3 solution. A yield larger than 100% can be explained by experimental error and/or dispensing inaccuracy during deposition of RbN_3 solution inside the cells.

3.7 Lifetime calculation

According to the Arrhenius equation, the Rb consumption rate (k) is temperature dependent (T) and depends on the activation energy (Ea) of the mechanism. Here, k is the Rb consumption rate, R is the ideal gas constant and A is a pre-factor with the same unit as 'k'.

$$k = Ae^{\frac{-E_a}{RT}}$$

Equation 6

By monitoring the Rb mass of the cells going though thermal aging, the Rb consumption rate at a certain temperature can be calculated. By performing accelerated aging tests at several temperatures and applying the Arrhenius relation, the activation energy of Rb consumption mechanism with a certain confidential level can be predicted.

By knowing the activation energy, as well as the consumption rate at a certain temperature, the lifetime of the MEMEs cells filled with a known amount of Rb can be calculated using the Arrhenius relationship, as shown below:

$$t_1 = t_2 exp[\frac{E_a}{R}\left(\frac{1}{T_2} - \frac{1}{T_1}\right)]$$

Equation 7

In which, t_1 is aging time at accelerated temperature T_1 and t_2 and T_2 are respectively operation time and temperature. R is the gas constant and E_a Is the activation energy for Rb loss mechanism.

For this project, the activation energy has been selected from the data measured in 2015, for a wafer containing 2 mm-diameter cells with Al_2O_3 layer deposited by MVD method as the barrier. Details about the selected approach is well explained in the work of Karlen *et al. [Vol. 25, No. 3 | 6 Feb 2017 | OPTICS EXPRESS 2187]*. In this work, a batch of 4 to 6 cells were aged at three different temperatures: 171°C, 185°C and 196°C over 7 months. The remaining amount of Rb inside the cells was calculated using monitoring method explained in section 3.3. afterwards, the averaged consumption rate of Rb were calculated using a linear fitting. The Rb consumption rate in an Arrhenius graph has been plotted in Figure 3-10. A linear regression fit on these data, results to the averaged value of the activation energy. The upper and lower limits for calculated and predicted interval of the Rb consumption rate has bene estimated using a statistical model. for these series of data, an activation energy of 67 ± 23 KJ/mol has been calculated. The uncertainty in the activation energy is estimated by considering 95% confidential level (predicted interval). This large uncertainty results in a large uncertainty of the cells lifetime as well.

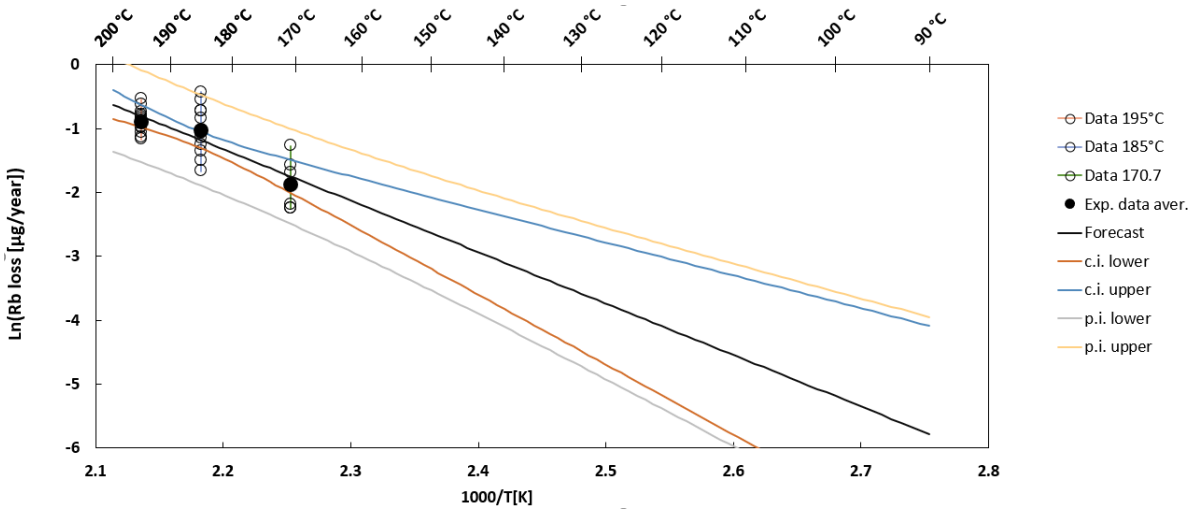

Figure 3-10: Arrhenius plot of the Rb consumption rate at three different aging temperatures.

3.7.1 Impact of h/a selection in lifetime calculation

In this report, two hypotheses have been considered for lifetime calculation:

1) Rb consumption rate (during accelerated aging) is linearly dependent on time.
2) Contact angle (h/a ratio) is constant for all cells

As previously explained (3.3), the volume and subsequently weight of metallic Rb droplets can be calculated from optically measured radius of Rb droplet (a) and contact angle (θ, or, h/a); as shown in Equation 8. In which K(θ) is a constant depending on h/a (nonlinearly) and Rb density.

$$Rb = a^3 * K(\theta) \qquad \textit{Equation 8}$$

Evaluation of Rb weight by time, during accelerated aging is given by Equation 9 and . Here, t is time and a(to) is the Rb droplet before accelerated aging.

$$Rb(t) = \frac{\Delta Rb}{\Delta t} \times t + Rb(t=0) \qquad \textit{Equation 9}$$

$$Rb(t) = \frac{\boldsymbol{K(\theta)}\left[a(t_2)^3 - a(t_1)^3\right]}{t_2 - t_1} \times t \; + \; K(\theta)\, a(t_0)^3 \qquad \textit{Equation 10}$$

The lifetime of the MAC cells is defined in a way zero Rb is left inside the cell as described in .

$$0 = \frac{K(\theta)\left[a(t_2)^3 - a(t_1)^3\right]}{t_2 - t_1} \times \boldsymbol{t_{life}} + \; K(\theta)\, a(t_0)^3 \qquad \textit{Equation 11}$$

By dividing both sides of by K(θ), cell lifetime can be estimated from **Error! Reference source not found.**.

$$t_{life} = \frac{-\,a(t_0)^3}{\frac{[a(t_2)^3 - a(t_1)^3]}{t_2 - t_1}}, \textit{ or, } t_{life} = \frac{-\,initial\ Rb\ amount}{slope} \qquad \textit{Equation 12}$$

These calculations clearly show the MAC cells lifetime is independent of the choice of contact angle as far as similar value of 'h/a' have been considered for both initial consumption and thermal aging consumption.

3.7.2 Lifetime calculation of ID20200616 cells

The accelerated aging was performed at 195°over 75 cells. The remaining metallic Rb was monitored optically inside each cell during accelerated testing and the results are presented in Figure 3-11.

The consumption rate of Rb at 195°C has been calculated for each cell by fitting a linear regression on data presented in Figure 3-11. In Figure 3-12(a) the histogram distribution of Rb consumption rate (µg/year) of ID20200616 cells at 195°C temperature is shown. Figure 3-12 (b) displays the cumulative distribution of the Rb consumption rate for these cells. In these calculations, a contact angle of 75° has been considered as explained in 3.4. A large scattering in the Rb consumption rate has been observed for ID20200616 series. The average value of Rb consumption rate at 195°C is listed in Table 1 for both Rb types: 87Rb and natRb. Here, the scattering in Rb consumption rate has been calculate from the standard deviation of the measured data.

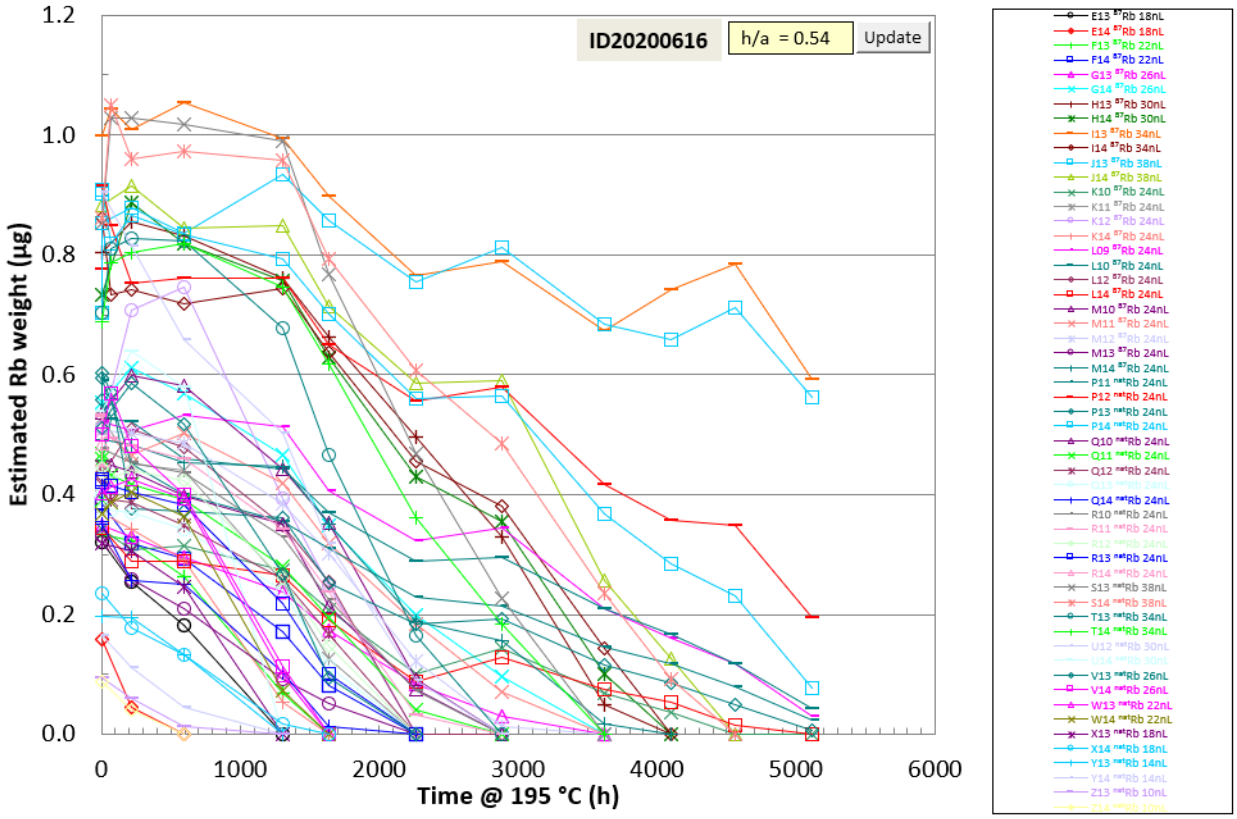

Figure 3-11: Optically estimated metallic Rb weight inside the MAC cells during thermal aging at 195°C.

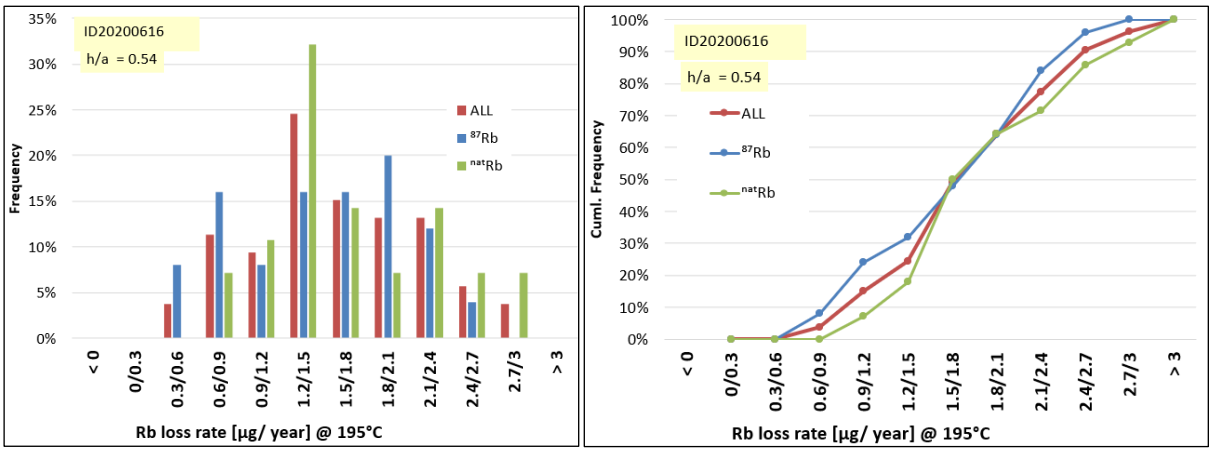

Figure 3-12: Histogram distribution and accumulative distribution of metallic Rb weight loss rate (µg/year) at 195°C aging temperature; calculated from optical images.

The consumption rate at operation temperature (95°C) has been extracted from the consumption rate at 195°C using Arrhenius equation and considering the activation energy determined from Figure 3-10. The results are listed in Table 1. The consumption rate at operation temperature has been calculated for both forecast and lower prediction level, while considering 95% confidential level. Data scattering (shown with ± in the graph) has been calculated from standard deviation of the Rb consumption rate at 195°C. For these calculations, following assumptions have bene considered:

1) The Arrhenius model is valid
2) The activation energy estimated between 170°C and 195°C is also valid for temperature range of 95°C to 170°C; the Rb consumption mechanism remains the same.
3) The activation energy estimated for 2mm diameter x 1mm cells, with MVD AlOx coating is valide as well for other cells, with different coating (i.e. ALD-AlOx), other dimensions (i.e. 3mm diameter x 1.5 mm) at the same temperature range
4) The statistical model used for calculation of the confidential level is applicable.

Table 1: the Rb consumption rate for IFD20200616 series at aging temperature of 195°C, operation temperature of 95°C (h/a=0.54, CONTACT ANGLE OF 57°).

Rb type	Average Rb consumption @195°C (µg/year)	Averaged Rb consumption @95°C (µg/10 year)	Averaged Rb consumption @ 95°C 95% confidence level, lower predicted interval (µg/10 year)
^{87}Rb	1.46± 0.57	0.18	0.8
^{nat}Rb	1.74± 0.72	0.21	0.95

The required N_2 pressure inside the cells for atomic clock application is equivalent of 61.706 mbar at 95°C. A decomposition yield and /or purity of 90% makes the required dispensing volume of RbN_3 solution inside the MAC cell equivalent to ~21 nl. Therefore, for contact angle of 57° selected for these series, by considering an AVERAGED Rb consumption rate (1.46 µg/year) and an AVERAGED Rb initial loss of (0.996 µg) for ^{87}Rb, the cells lifetime is estimated between 3 and 90 years (with 95% predicted interval level), with an average value of 16 years. These values are listed in Table 2.

Table 2: lifetime estimation of ID20200616 MAC cells, with 3 mm diameter and ALD- AlOx coating. Zje upper and limits have been calculated using 95% confidential level.

contact angle =	57°
Initial ^{87}Rb loss [µg]	1.00
Test temperature [°C]	195.00
^{87}Rb Rb loss @ 195°C [µg/year]	1.46
Cell operating temperature [°C]	95.00
Rb type	^{87}Rb
Required N_2 pressure at 95°C [mbar]	61.71
N_2 pressure at 23°C [mbar]	49.64
^{87}Rb produced by RbN_3 decomposition [µg]	1.22
Yield (UV and/or purity)	0.90
Dispensing volume taking into account the 87% yield [nL]	20.88
Remaining metallic Rb [µg]	0.22
Predicted lifetime [year]	16.30
Predicted lifetime [year] - 95% confidence level lower estimate	2.88
Predicted lifetime [year] - 95% confidence level higher estimate	92.31

4 Next steps: reduction of the lifetime estimation uncertainty

The large range in the estimated lifetime of MAC cells originates from two sources:

1) Significant scattering in the MAC cells behavior and Rb consumption rate (^{87}Rb: 1.46± 0.57 µg/ year)
2) Large uncertainty in the estimated value of activation energy for 95% confidential level (67 ± 23 KJ/mol)

The scattering in Rb consumption depends on fabrication process and RbN_3 dispensing accuracy (filling process). On the other hand, the uncertainty in the estimated value of activation energy can be improved by adding more measured data to the existing Arrhenius graph in Figure 3-10. For this purpose, accelerated aging will be performed at two extra temperatures: 160° C and 110° C. The proposed test plans for both 2mm and 3mm diameter cells are described in Figure 4-1 and Figure 4-2.

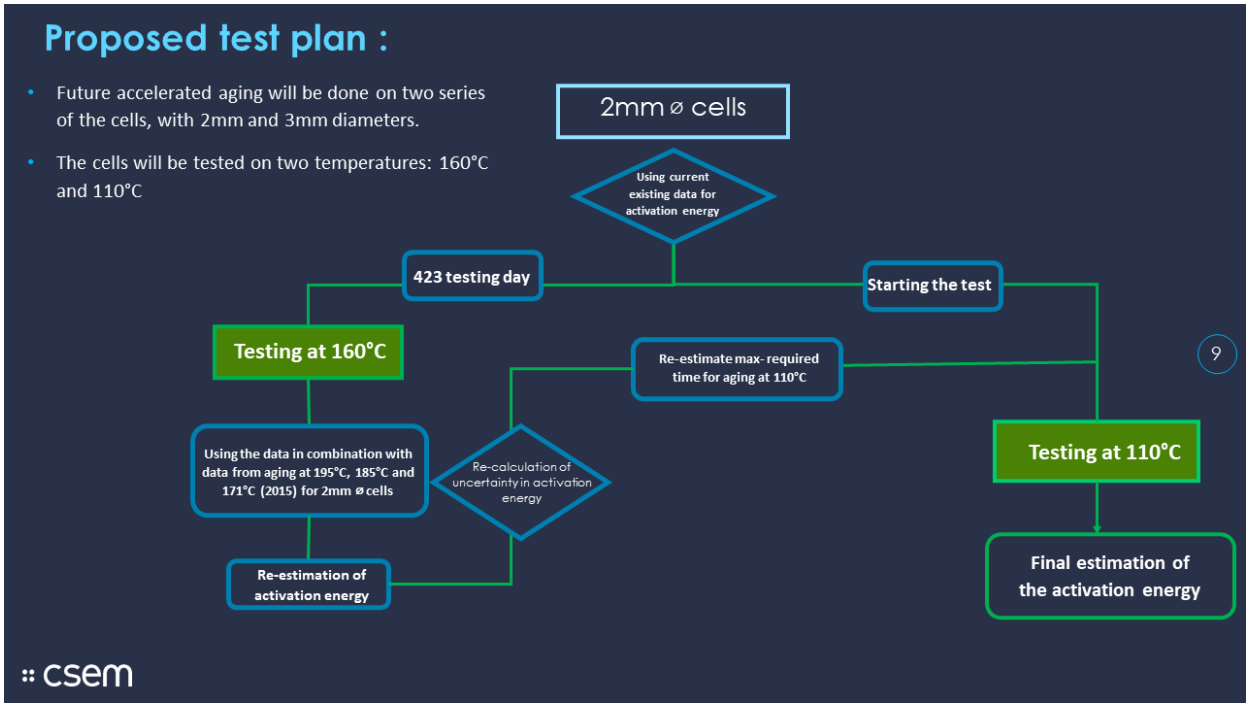

Figure 4-1: Proposed test plan for 2mm diameter cells.

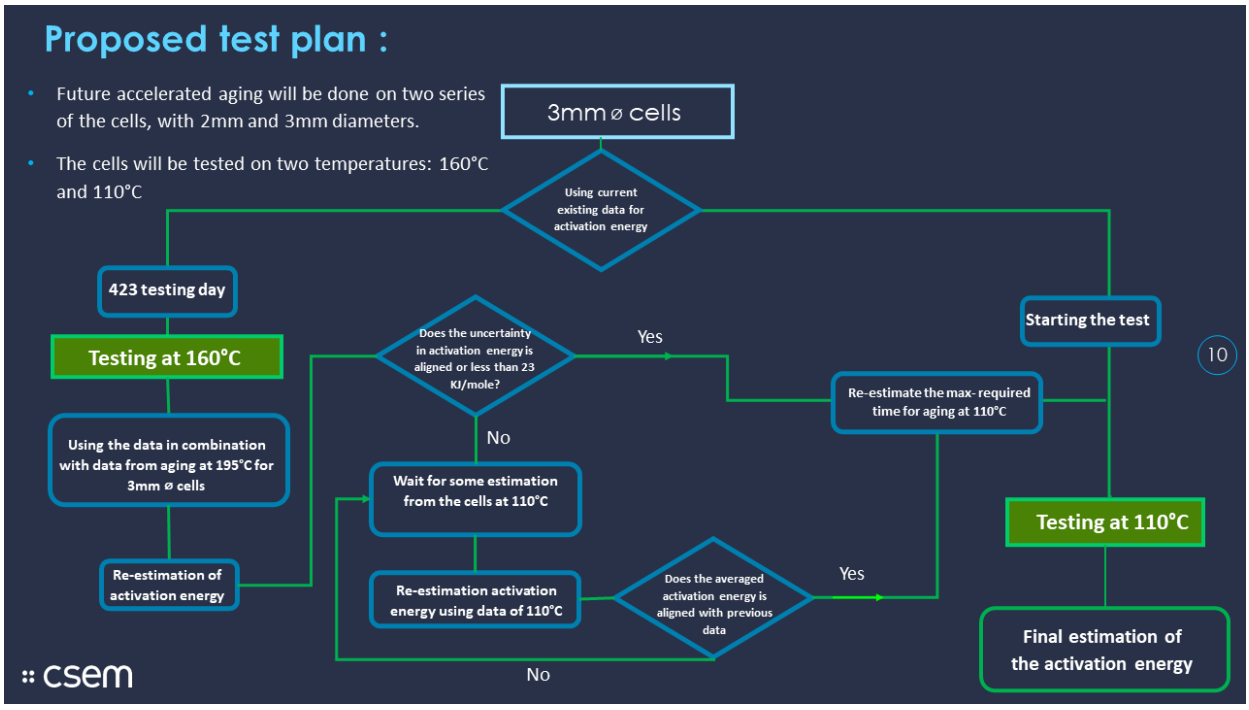

Figure 4-2: Proposed test plan for 3mm diameter cells.

5 Drift measurement

Characterization of the atomic vapor cells and estimation of their lifetime (previous chapters) are key aspects for the atomic vapor cells to be at once validated for a commercial product. The fabrication processes will also need to be up scaled and validated before commercialization.

In order to already assess the potential of these atomic vapor cells for miniature clock applications, a commercial compact clock from Orolia Switzerland SA (mRO-50[1], Figure 5-1) was modified so as to be able to integrate the MEMS atomic vapor cells developed in macQsimal in place of a cylindrical glass blown cell.

Figure 5-1: mRO-50[1] commercial clock from Orolia Switzerland SA.

The mRO-50[1] compact clock illustrated in Figure 5-1 uses a cylindrical glass blown cell as the Rubidium container. Orolia Switzerland SA has modified three mRO-50 units in a way that MEMS atomic vapor cells could be integrated as a replacement of the glass blown cell.

Figure 5-2 shows how the MEMS atomic vapor cells were glued in place within the cylindrical heater of the mRO-50.

[1] http://www.orolia.com/products/atomic-clocks-oscillators/mro-50

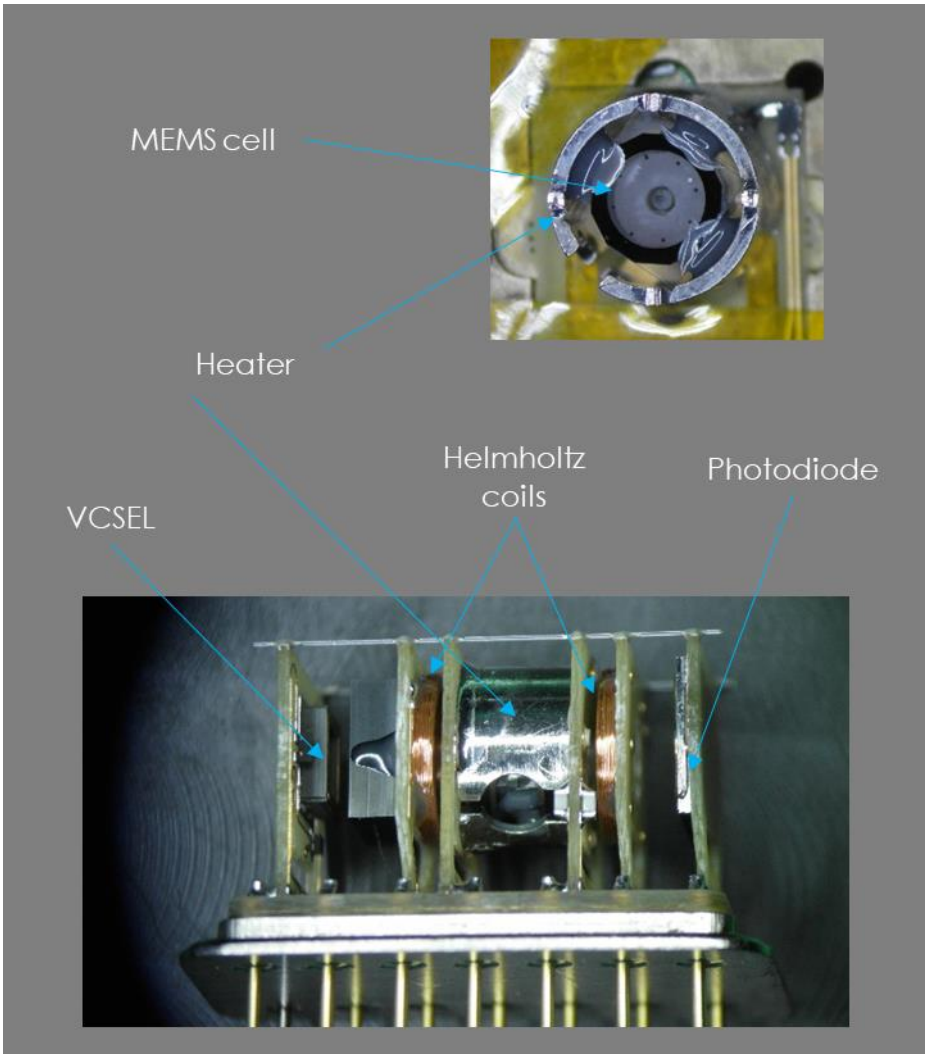

Figure 5-2: Modified mRO-501 clocks in which a MEMS atomic vapor cell replaces the glass blown cell.

Once modified, the three modified mRO-50 units were encapsulated and functional tested. The clock parameters were optimized for the MEMS atomic vapor cell, mainly the temperature of it, in order to get the best possible performance while keeping the other parameters as close as possible to the parameters used by the mRO-50 when it is operated with a glass cell.

The output frequency of the three clocks was monitored in order to extract the frequency drift performance. This drift is mainly due to the new integrated MEMS cells.

The requirement for the MEMS atomic vapor cell is a relative frequency drift below $1 \cdot 10^{-11}$/ day. As can be seen in Figure 5-3, after 430 days of measurements, all three devices showed frequency drift below $5 \cdot 10^{-12}$/ day, so already much better than the requirement. Figure 5-3 also illustrated the aging of the cells. It is well known in the field that cell based atomic clock need time to stabilize before being sold and achieve their expected performance. The monitoring will be prolongated and the reduction of frequency drift will continue. Frequency drifts below $2 \cdot 10^{-12}$/ day are expected for all cells, performances which are at the same level as standard glass blown cells. MEMS atomic vapor cells are thus validated and compatible with miniature atomic clock requirements.

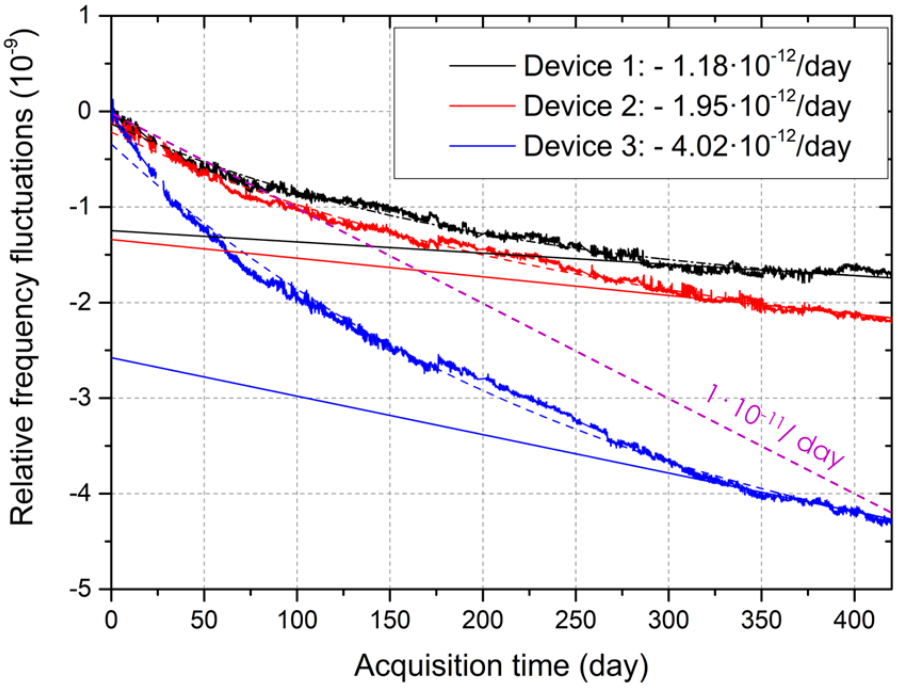

Figure 5-3: Relative frequency drift of the three mRO-50 clocks modified for MEMS cells.

6 Conclusion

Different techniques, including optical microscopy and Raman spectroscopy are employed for characterization and lifetime estimation of the vapor cells filled with rubidium produced by UV decomposition of RbN_3. N_2 partial pressure inside the cells with different RbN_3 filling quantities is measured using Raman spectroscopy. Comparison between the measured value and the theoretical value of N_2 pressure gives an estimation of the solution's purity as well as the UV-decomposition yield. A purity/ decomposition yield of 95.6% ± 5.8% and 88.8% ± 9% is estimated respectively for cells containing ^{87}Rb and nat-Rb.

The initial and the in-operation consumption of rubidium are considered as the main failure mechanisms of the cells. To estimate the lifetime, the in-operation consumption is considered as a temperature dependent factor with a fixed rate following an Arrhenius law, while initial loss remains independent of the temperature and time. Both Rb initial loss and Rb consumption rate (at 195°C) are estimated from optical monitoring of the metallic Rb droplets forming up on the cell top window. The activation energy related to the Rb in-operation consumption was estimated as 67 ± 23 KJ/mol for cells with Al_2O_3 coating.

The required N_2 pressure of 61.7 mbar (at 95°C) for vapor cells used in MAC combined with a decomposition/purity of 90%, makes the required dispensing volume of RbN_3 solution inside the vapor cell equivalent to approximately 21 nl. This calculation is correct only for the cells with dimension of 1.5mm height x 3mm diameter and with Al_2O_3 diffusion barrier on the surface. For a contact angle of 57°, an AVERAGED Rb consumption rate (1.46 µg/year) and an AVERAGED Rb initial loss of (0.996 µg) are calculated for vapor cells containing ^{87}Rb. For these cells, the lifetime is estimated between 3 and 90 years (with 95% predicted interval level), with an average value of 16 years (forecast value).

Relative frequency drifts of the MEMS atomic vapor cells were shown to meet the miniature atomic clock requirements by integrating such cells in commercial clocks. The MEMS cells approach has thus been validated.